Electronic Supplementary Information

An *in situ* Approach for Facile Fabrication of Robust and Scalable SERS Substrates

Yi-Chung Wang,[a] Joseph S. DuChene,[a] Fengwei Huo,[b] and Wei David Wei[a*]

[a] Department of Chemistry and Center for Nanostructured Electronic Materials, University of Florida, Gainesville, FL 32611, USA

[b] Jiangsu-Singapore Joint Research Center for Organic/Bio-Electronics & Information Displays and Institute of Advanced Materials (IAM), Nanjing Tech University, 30 South Puzhu Road, Nanjing 211816, China

Contents:

* Fax: +1-352-392-0872; Tel: +1-352-392-2050; E-mail: wei@chem.ufl.edu

(a) Digital image of PDMS pyramids substrate

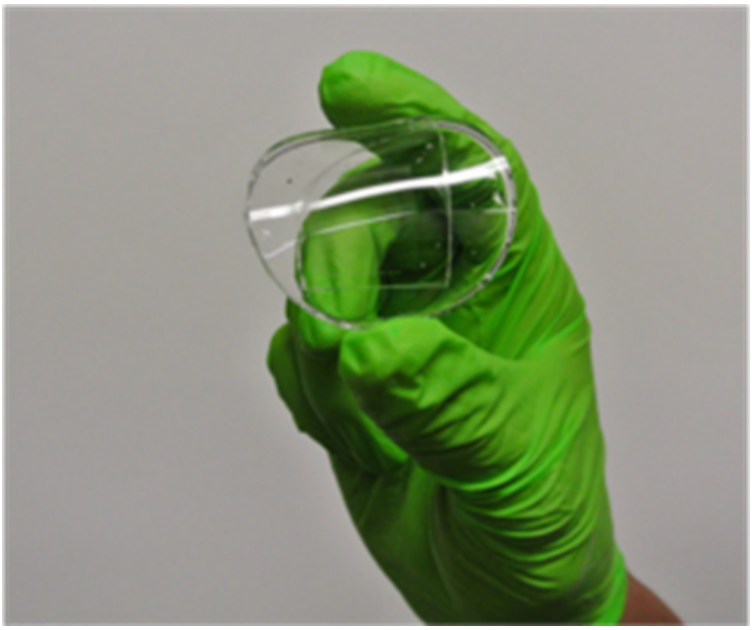

Fig. S1 A digital image of the PDMS pyramids substrate after peeling it off from the Si wafer, demonstrating the mechanical flexibility of the substrate.

(b) Elemental analysis of the Au/p-PANI/PDMS substrate

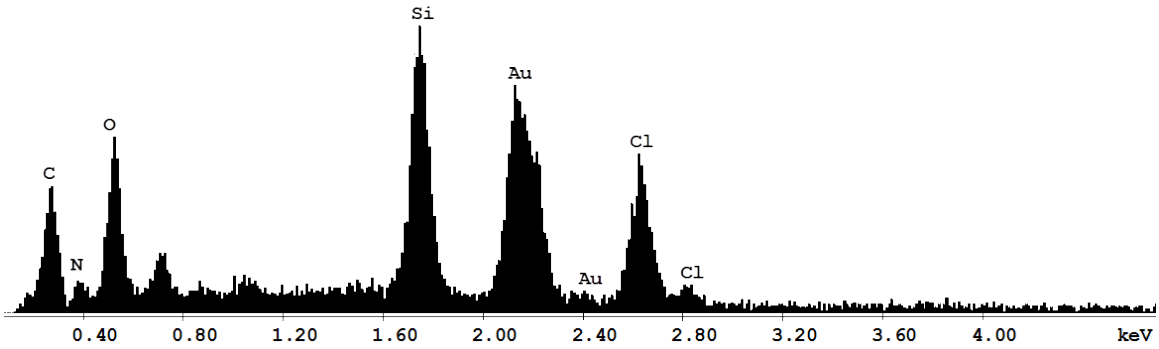

Fig. S2 Elemental analysis of the Au/p-PANI/PDMS substrate by EDS.

The energy dispersive x-ray spectroscopy (EDS) spectrum was collected under 20,000x magnification with an accelerating voltage of 10 kV. The area of the signal collection covers only one pyramid, corresponding to Fig. 2c. It is clear that Au was deposited on the substrate. The relatively strong peak of Cl may be due to the residue of $HAuCl_4$ solution.

(c) X-ray diffraction pattern of of Au nanoparticles on p-PANI/PDMS substrates

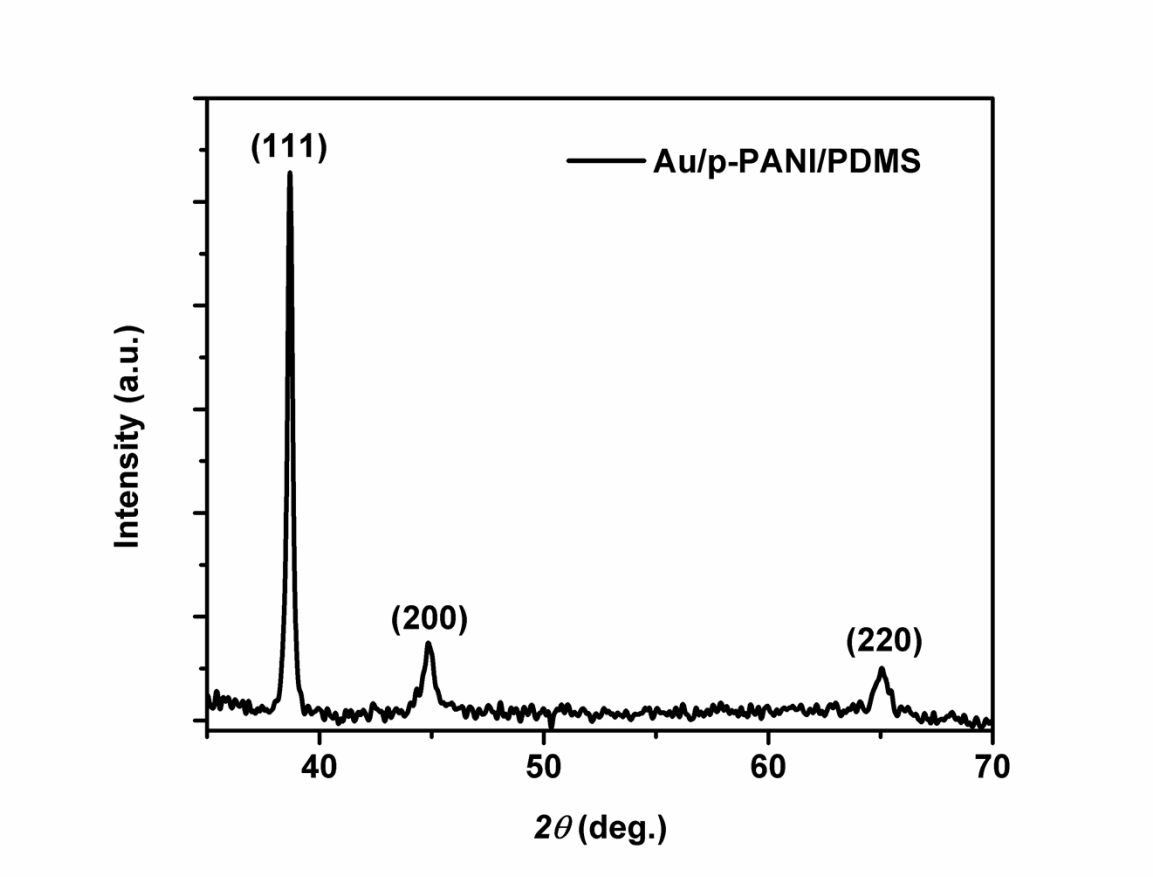

Fig. S3 XRD result of Au NPs grown on a p-PANI/PDMS substrate.

The diffraction peaks can be indexed to Au (111), (200), and (220) crystal planes,[1, 2] showing that the reduced Au NPs on p-PANI belong to the face-centered-cubic (fcc) crystal lattice. Notably, the higher intensity ratio of (111)/(200) (~ 7.1) to that of a bulk thin film (~ 2.8-5.0) deposited by PVD suggests that the Au NPs are preferentially oriented along the Au (111) growth direction.[1, 3]

(d) Optical characterization

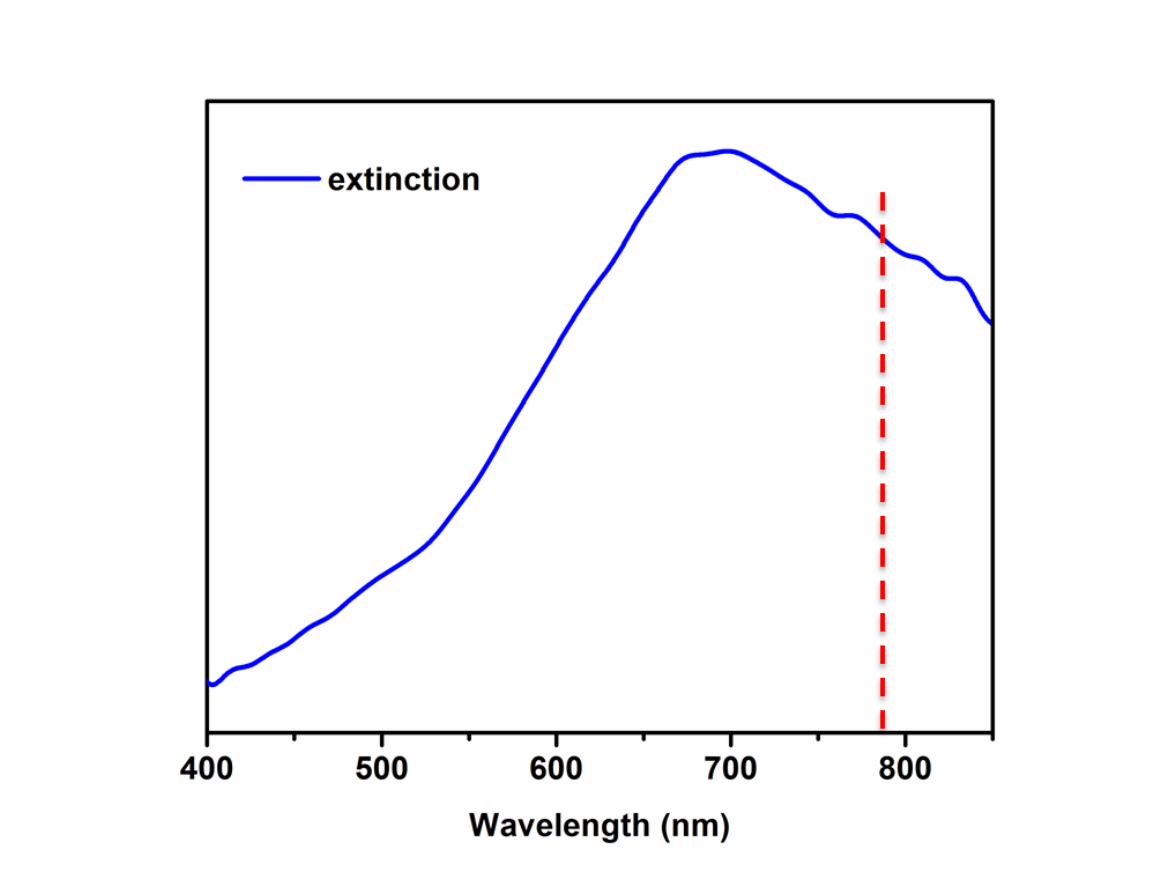

Fig. S4 The extinction spectrum for a typical Au pyramid structure.

The maximum extinction cross section is located around 700 nm. A 785 nm laser was chosen as the excitation source to prevent direct laser excitation of the Raman probe molecules, while still allowing for sufficient excitation of the Au pyramid for the Raman measurements.

(e) Additional Raman mapping results

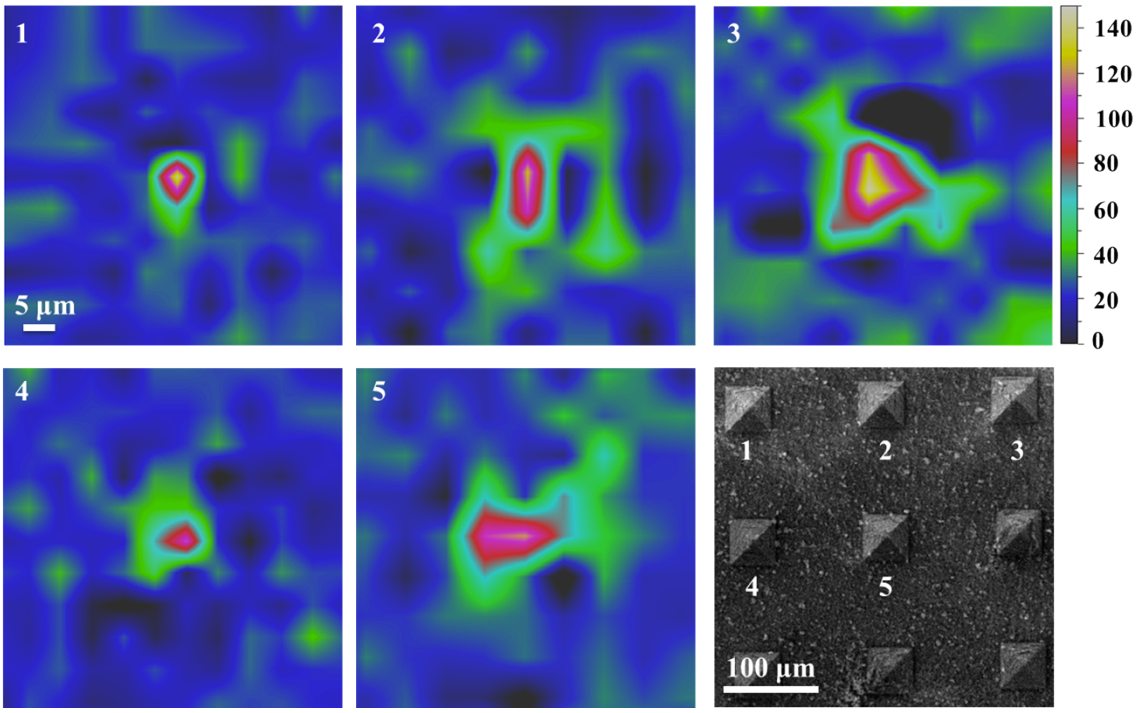

Fig. S5 Raman mapping results obtained from pyramids 1 to 5, demarcated by the number marked on the SEM image.

Due to current instrument limitations, direct Raman mapping over a large area for our substrate with a 10x objective lens was not attainable because we were unable to prevent slight stage movement while mapping such a large area. Therefore, instead of using a 10x objective lens, a 50x objective lens was used to map a 55×55 μm^2 area, which covers a pyramid and the nearby flat film. It can be seen in Fig. S5 that the pyramid tips always have higher Raman intensities than the adjacent films, demonstrating the reproducibility of these plasmonic substrates for SERS.

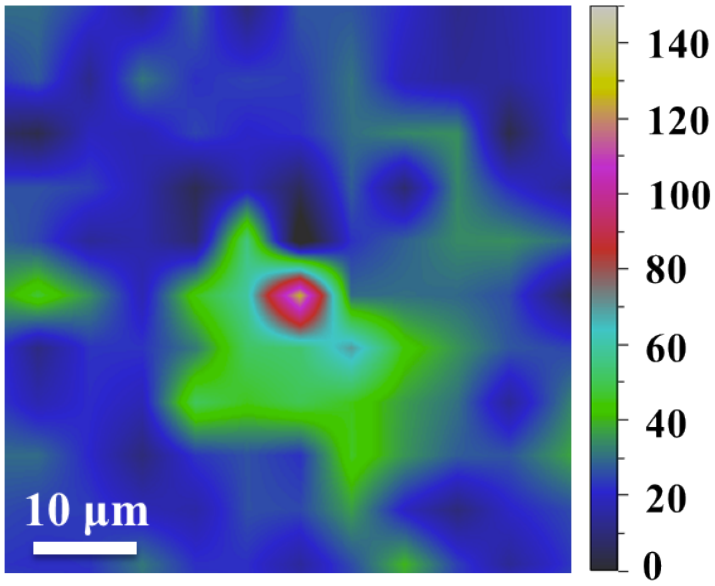

Fig. S6 Raman mapping of pyramid 1 after folding the substrate thirty times and taken three months after the initial measurement.

The fabrication starts with a lithographic method that provides precise alignment of Au pyramid arrays. We could track the position of each pyramid in accordance with the SEM image and the optical image in the Raman system. Fig. S6 demonstrates the mapping results of pyramid 1 after bending the substrate thirty times and taken three months after the initial measurement. Compared to Fig. 3b, it is apparent that not only does the tip still show the highest intensity, but also that the intensity is very similar to the result before folding. The difference in intensity distribution between two mappings could be due to the slight focus mismatch in two measurements.

(f) Discussion of SERS spectrum

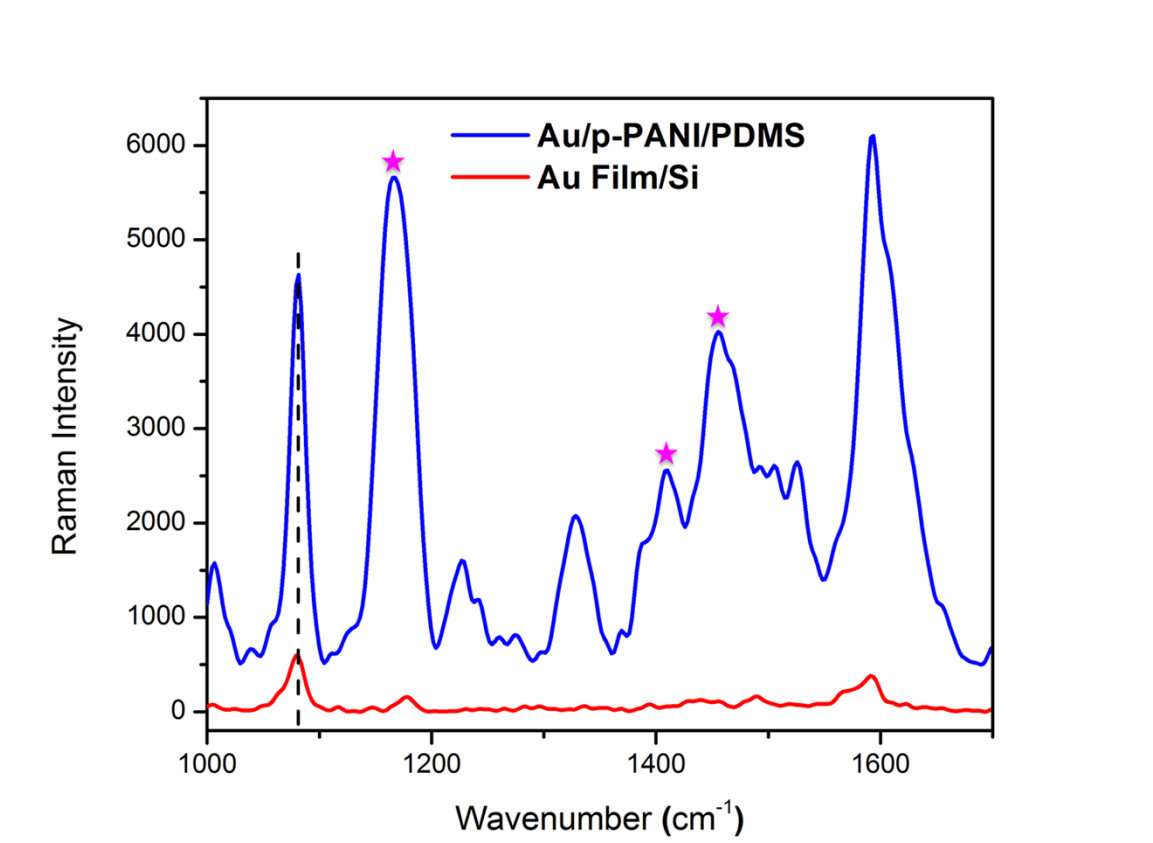

Fig. S7 SERS measurements on the Au/p-PANI/PDMS substrate and on a 30 nm Au flat film fabricated by e-beam evaporation. The dashed line indicates the peak used to calculate the SERS enhancement factor in the next section.

Three peaks indicated by the pink stars belong to the C-H bending mode of PANI vibrations. The ratio of peaks at 1417 cm^{-1} and 1455 cm^{-1} can be used to confirm the emeraldine salt structure of polyaniline.[4, 5] The PANI signal is due to discontinuities in the Au film, and the Raman features of p-PANI could also be enhanced by the Au NPs.

(g) Calculation of SERS enhancement factor

The SERS enhancement factor was calculated based on the following equation[6]:

$$EF = \frac{I_{sers}}{I_{bulk}} \frac{N_{bulk}}{N_{sers}}$$

where I_{sers} and I_{bulk} are the SERS intensity and non-enhanced Raman intensity of the band at 1079 cm^{-1} (dashed line in Fig. S6), respectively. N_{sers} and N_{bulk} are the numbers of Raman molecules on the surface that were excited in the vicinity of the local field and within the bulk illumination volume (non-enhanced sample), respectively. We adopt the packing density (6.8×10^{14} molecules/cm^2) and the density (1.073 g/cm^3) of liquid 4-aminobenzenethiol from previous reports[7, 8] to calculate N_{sers} and N_{bulk}. Here, the focus volume of the 785 nm laser was estimated by taking into account that the size of the measured laser spot is ~2 μm in diameter, and that the penetration depth into 4-ABT is ~40 μm, taken from a prior report.[9] The surface area of the enhanced Raman signal is calculated by $A_{surf} = d^2$, where d is the edge length of the pyramid tip, assuming a perfect square. Accordingly, the estimated N_{bulk} is 1.76×10^{13}, and N_{sers} is 1.7×10^{6}. The acquisition time for the flat film is 10 s and for the Au/p-PANI/PDMS substrate is 5 s.

References:

1. K. Uosaki, Y. Shen and T. Kondo, *J. Phys. Chem.*, 1995, **99**, 14117-14122.
2. X. Chen, Y. Wang, J. Zhou, W. Yan, X. Li and J.-J. Zhu, *Anal. Chem.*, 2008, **80**, 2133-2140.
3. A. Gupta and D. K. Avasthi, *Phys. Rev. B*, 2001, **64**, 155407.
4. R. A. Davidson and T. Guo, *J. Phys. Chem. Lett.*, 2012, **3**, 3271-3275.
5. M. Baibarac, M. Cochet, M. Lapkowski, L. Mihut, S. Lefrant and I. Baltog, *Synth. Met.*, 1998, **96**, 63-70.
6. K. A. Willets and R. P. Van Duyne, *Annu. Rev. Phys. Chem.*, 2007, **58**, 267-297.
7. Q. Yu, P. Guan, D. Qin, G. Golden, P. M. Wallace, *Nano Lett.,* 2008, **8**, 1923-1928.
8. Z. Q. Tian, B. Ren, D. Y. Wu, *J. Phys. Chem. B,* 2002, **106**, 9463-9483.
9. K. Kim, D. Shin, H. B. Lee, K. S. Shin, *Chem. Commun.,* 2011, **47**, 2020-2022.